

# The BH-PSR Gravitational Molecule

Tao Liu<sup>1,\*</sup> and Kun-Feng Lyu<sup>1,†</sup>

<sup>1</sup>*Department of Physics and Jockey Club Institute for Advanced Study,  
The Hong Kong University of Science and Technology, Hong Kong S.A.R., China*

While an axion-clouded black hole (BH) encounters a pulsar (PSR) or has a PSR companion, a “gravitational molecule” can be formed. In such a system, the axion cloud evolves at the binary hybrid orbitals, as it happens at microscopic level to electron cloud in a chemical molecule. To demonstrate this picture, we develop a semi-analytical formalism using the method of linear combination of atomic orbitals with an adiabatic approximation. An oscillating axion-cloud profile and a perturbed binary rotation, together with unique and novel detection signals, are then predicted. Remarkably, the proposed PSR timing and polarization observables, namely the oscillation of periastron time shift and the birefringence with multiple modulations, correlate in pattern, and thus can be properly combined to strengthen the detection.

**Introduction** — “Superradiance” of bosons can occur near a spinning black hole (BH) [1–11], if their Compton wavelength is bigger than the BH horizon. Then certain energy levels of this BH get populated with these ultralight bosons, by extracting its own angular momentum and energy. Eventually a “gravitational atom” with a BH “nucleus” is formed. Here  $|211\rangle$  [7], namely a level with gravitational principal, orbital and magnetic quantum numbers  $\{n = 2, l = 1, m = 1\}$ , may serve as a leading state. This mechanism of interplaying the ultralight bosons and a spinning BH has been known for decades.

Among the set of the ultralight-boson candidates, axion is especially interesting. Axion is originally proposed to solve the strong CP problem [12–18]. This concept is later generalized to some ultralight bosons in new physics and string theory [19–21]. The axions and axion-like particles (we will not distinguish them below) can serve as a primary component of dark matter in the universe, with a mass ( $m_\phi$ ) ranging from sub eV to  $\sim 10^{-22}$  eV [22]. So far, various astrophysical and cosmological probes for its detection have been proposed (see, e.g., [23]).

The advent of multi-messenger astronomy provides a great opportunity to investigate gravitational atoms and explore the physics of ultralight bosons, which has motivated extensive studies in literatures (see, e.g., [24–39]). Recently, the study was extended to gravitational-atom binaries, with their companion being either a BH [40–42] or a pulsar (PSR) [35, 43]. Especially, the Landau-Zener energy-level transitions induced by the companion’s perturbation have been suggested to be a probe for gravitational atoms (or “gravitational collider” physics) [42–46].

In this letter, we will study a novel gravitational system noticed recently [47] - “gravitational molecule”. While a gravitational atom encounters a BH or a neutron star (NS) or has such a massive companion, a gravitational molecule can be formed. The axion cloud from this atom will (partly) flow to its companion, along their hybrid orbitals. This mechanism is generically different from the mass transfer of Type Ia supernova binaries: (1) the axion cloud is generated as a coherent field while the transferred matter in the latter case is particle-like; and

(2) the flow can occur to the axion cloud in Roche lobe, where no Newtonian matter transfer takes place, due to orbital hybridization. Such a system thus can be viewed as a macroscopic counterpart of a diatomic molecule.

To demonstrate this picture, we will develop a semi-analytical analysis formalism, and apply it to the BH-PSR molecules. This formalism can be applied to the BH-BH molecules also. The specification of a PSR as the companion is because the BH-PSR binaries are expected to be future precision astronomical laboratories. According to recent estimations [48–50], in our galaxy  $\sim \mathcal{O}(10^{-10^3})$  BH-PSR binaries are yet to be discovered. The study of such a gravitational molecule may benefit from not only its gravitational-wave (GW) signals, but also the PSR timing/polarization signals. Recall, in history the timing signals of PSR B1913+16 have provided the first evidence on GWs [51–53]. So, a BH-PSR molecule will be highly valuable for multi-messenger astronomy.

Yet, precisely analyzing the physics of such a gravitational molecule is very involved. In quantum chemistry, numerical tools are usually applied. Here we will take a semi-analytical method instead. We will model this molecule in a simplified way, analyze its orbital hybridization and state evolution using the method of linear combination of atomic orbitals (LCAO) [54] with an adiabatic approximation, and then explore its astronomical detection signals. This methodology allows us to explore typical or generic aspects of gravitational molecules without involving much numerical work. We would view it to be a starting point for more refined analyses later.

**Modeling the BH-PSR Molecule** — To simplify the analysis, we model the BH-PSR molecule with a series of assumptions. At  $t \leq 0_-$ , the atomic BH stays in an initial state of  $|211\rangle$ , with the PSR’s gravitational perturbation being negligibly small. Here the BH “Bohr radius” and “fine-structure constant” are given by [44]

$$\begin{aligned} r_c &= \frac{1}{m_\phi \alpha} = 1.3 \times 10^4 \times \left( \frac{0.015}{\alpha} \right) \left( \frac{10^{-12} \text{eV}}{m_\phi} \right) \text{ km} , \\ \alpha &= GM_{\text{BH}} m_\phi = 0.015 \left( \frac{M_{\text{BH}}}{2M_\odot} \right) \left( \frac{m_\phi}{10^{-12} \text{eV}} \right) . \end{aligned} \quad (1)$$

A percent-level  $\alpha$  is then obtained for  $m_\phi \sim 10^{-12}$  eV and  $M_{\text{BH}} \sim M_\odot$ . In this case, the depletion of the axion cloud by emitting the GWs occurs at a cosmic time scale. The caused mass loss thus can be neglected. We also assume the BH's angular velocity at its outer horizon to be

$$\Omega_{\text{BH}} < \frac{E_{211}}{m} \sim m_\phi. \quad (2)$$

Here  $E_{211}$  is the  $|211\rangle$  eigenenergy. This condition implies that no more axions will be produced by superradiance.

At  $t = 0_+$ , the axion cloud starts to evolve at the hybrid orbitals of this molecule, where the BH atom and its companion is separated with  $R = R_0$ . This assumption models the diabatic formation of gravitational binaries by, e.g., three-body exchange [55–62] (one of the main mechanisms for binary production by which, especially, most stellar BH-BH binaries in star clusters may have been produced [60–62]). Its application can be also extended to the molecules with a prompt orbit shrinking (from  $R = R'_0$  to  $R = R_0$  with  $R'_0 > R_0$ , at  $t = 0_+$ ) caused by either three-body hardening [55, 62, 63] or resonant level transition [45], where the axion-cloud initial state is defined at  $R = R'_0$ . The binary rotation, which we assume to be circular (with an angular velocity  $\omega = |\boldsymbol{\omega}| = \frac{2\pi}{T_b} = \omega_i$  initially) and anti-parallel to the BH spin for concreteness, will be perturbed by the axion-cloud evolution then. Notably, a fully-occupied  $|211\rangle$  state has total energy  $M_{\text{AC}} \sim Nm_\phi$  with the occupation number  $N \sim [10f_\phi/(\alpha^{3/2}m_\phi)]^2$  being set by Bosenova limit [64]. Here  $f_\phi$  is axion decay constant. Assuming  $M_{\text{BH}} = M_{\text{PSR}} = M$  (the BH and the PSR then share the  $\alpha$  and  $r_c$  values), we have

$$\varepsilon = \frac{M_{\text{AC}}}{M} \lesssim \frac{m_e}{m_p} \ll 1 \quad (3)$$

for  $M \sim M_\odot$  and  $f_\phi \lesssim 10^{13}$  GeV at  $m_\phi = 10^{-12}$  eV [65]. This implies that, given the same amount of kinetic energy, the relative change to the BH-PSR motion is much smaller than that of the axion cloud. So, this analysis can be pursued with an adiabatic approximation.

In the spirit of Born-Oppenheimer approximation in quantum chemistry, we separate our analysis to two steps. We first analyze the axion-cloud evolution using the LCAO method, with the BH-PSR rotation being assumed to be unperturbed. Then we apply the conditions of angular-momentum and energy conservation to solve the perturbation to the BH-PSR rotation. Here the first part is modeled as a quantum-mechanics problem with a time-dependent potential, while the second one is “classical”, since the binary quantum effects are tiny.

The coordinate system for the rotating reference frame of this BH-PSR molecule is demonstrated in Fig. 1, where the original point is positioned at the BH-PSR mass center, and the  $x$ - and  $z$ -axes are defined by the BH-PSR line and the BH spinning direction, respectively. The axion

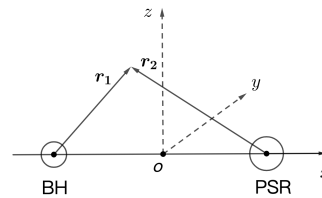


FIG. 1: Coordinate system for the rotating reference frame of the BH-PSR molecule.

cloud, as a real scalar field, is given by

$$\phi(t, \mathbf{r}) = \frac{1}{\sqrt{2m_\phi}} [\psi(t, \mathbf{r}) \exp(-im_\phi t) + \text{h.c.}] . \quad (4)$$

Here  $\psi$  is complex and satisfies gravitational Schrodinger equation (up to some higher-order curvature corrections)

$$i \frac{\partial}{\partial t} \psi(t, \mathbf{r}) = \left( \frac{\mathbf{p}^2}{2m_\phi} + V_1 + V_2 + V_c \right) \psi(t, \mathbf{r}) , \quad (5)$$

where  $V_{1,2} = -\alpha/|\mathbf{r}_{1,2}|$  are the BH and the PSR gravitation potentials, and  $V_c = -\boldsymbol{\omega} \cdot \mathbf{L} = -\boldsymbol{\omega} \cdot (\mathbf{r} \times \mathbf{p})$  is the inertia potential of the axion cloud arising from the binary rotation [66]. All of them are of order  $\sim \mathcal{O}(\alpha^2)$  in the length unit of  $r_c$  (note  $\omega = (2GM/R^3)^{1/2} = \sqrt{2}\alpha^2 m_\phi / (R/r_c)^{3/2}$ ). The Coriolis and centrifugal forces will appear in the Heisenberg equation of  $\mathbf{r}$  then. Interestingly, by mapping  $\{-\frac{1}{2}(\boldsymbol{\omega} \times \mathbf{r})^2, \boldsymbol{\omega} \times \mathbf{r}\}$  to the four-vector potential and hence  $\{\boldsymbol{\omega} \times (\mathbf{r} \times \boldsymbol{\omega}), \boldsymbol{\omega}\}$  to  $\{\mathbf{E}, \mathbf{B}\}$  [67], one can find this non-relativistic system to be an analog to chemical molecule in an electromagnetic field. At last, for  $R < 5r_c$  the radius of Roche lobe (at Lagrange-point-2 side) [68] becomes  $< 2r_c$ , at which the initial axion-cloud distribution is expected to be peaked. Part of the axion cloud might be pushed far away from the binary then. So, our study will focus on the scenario with  $R > 5r_c$ .

#### Orbital Hybridization and State Evolution

We introduce a basis for  $n_i = 2$  atomic states ( $i = 1, 2$ ) is a shorthand notation for “BH” and “PSR”):  $|s_i\rangle = |200, i\rangle$  and  $|p_{x,i}\rangle = (|211, i\rangle - |21 - 1, i\rangle)/\sqrt{2}$ ,  $|p_{y,i}\rangle = (|211, i\rangle + |21 - 1, i\rangle)/\sqrt{2}i$ . Here  $|s_i\rangle$  is spherically symmetric in space, while  $|p_{x(y),i}\rangle$  is aligned with the  $x(y)$ -axis. Note,  $|p_{z,i}\rangle$  is irrelevant here since it does not couple with the others via the Hamiltonian. Then we can define a hybrid basis, including the  $s_1 - s_2$  bond ( $\sigma_s$ ) and anti-bond ( $\sigma_s^*$ ), the  $p_x - p_x$  bond ( $\sigma$ ) and anti-bond ( $\sigma^*$ ), and the  $p_y - p_y$  bond ( $\pi$ ) and anti-bond ( $\pi^*$ ). Explicitly we have

$$\begin{aligned} |\sigma_s\rangle &= A_{\sigma_s} (|s_1\rangle + |s_2\rangle), & |\sigma_s^*\rangle &= A_{\sigma_s^*} (|s_1\rangle - |s_2\rangle), & (6) \\ |\sigma\rangle &= A_\sigma (|p_{x,1}\rangle + |p_{x,2}\rangle), & |\sigma^*\rangle &= A_{\sigma^*} (|p_{x,1}\rangle - |p_{x,2}\rangle), \\ |\pi\rangle &= A_\pi (|p_{y,1}\rangle + |p_{y,2}\rangle), & |\pi^*\rangle &= A_{\pi^*} (|p_{y,1}\rangle - |p_{y,2}\rangle), \end{aligned}$$

with the normalization coefficients

$$A_{\sigma_s, \sigma, \pi} = \frac{1}{\sqrt{2(1 + S_{s,x,y})}}, \quad A_{\sigma_s^*, \sigma^*, \pi^*} = \frac{1}{\sqrt{2(1 - S_{s,x,y})}}. \quad (7)$$

Here  $S_s = \langle s_1 | s_2 \rangle$ ,  $S_x = \langle p_{x,1} | p_{x,2} \rangle$  and  $S_y = \langle p_{y,1} | p_{y,2} \rangle$  are overlap integrals of  $s$ ,  $p_x$  and  $p_y$ , respectively. The axion-cloud initial state is then given by

$$\begin{aligned} |211,1\rangle &= \frac{\sqrt{2}}{2} (|p_{x,1}\rangle + i|p_{y,1}\rangle) \\ &= \frac{1}{2\sqrt{2}} \left( \frac{|\sigma\rangle}{A_\sigma} + \frac{|\sigma^*\rangle}{A_\sigma^*} + i \frac{|\pi\rangle}{A_\pi} + i \frac{|\pi^*\rangle}{A_\pi^*} \right). \end{aligned} \quad (8)$$

For the convenience, below we will analyze the orbital hybridization in the hybrid basis, and study the  $\phi(t, \mathbf{r})$  profile and the relevant physics in the atomic basis.

In quantum chemistry, the  $2s$ - $2p$  orbital hybridization is often ignored for homonuclear diatomic molecules such as  $O_2$  and  $F_2$ , for the relatively big  $2s$ - $2p$  energy-level splitting. But, this does not apply well here, since  $|\langle \sigma_s(\sigma) | V_1 + V_2 | \sigma(\sigma_s) \rangle| > |\langle \sigma_s | V_1 + V_2 | \sigma_s \rangle - \langle \sigma | V_1 + V_2 | \sigma \rangle|$ . This is reminiscent of some other period-2 diatomic molecules such as  $N_2$  and  $C_2$ , where Coulomb repulsion from the  $\sigma$  electrons reduces the  $2s$ - $2p$  energy-level splitting and hence results in a non-trivial  $2s$ - $2p$  hybridization. Yet, the case for this BH-PSR molecule is even more complicated. The axion-cloud inertia potential correlates the BH-PSR  $\sigma(\sigma^*)$  and  $\pi^*(\pi)$  states, because of  $\langle \pi^*(\pi) | V_c | \sigma(\sigma^*) \rangle \neq 0$ . This effect breaks  $\sigma$  symmetry (a cylindrical symmetry about the  $x$ -axis) and hence yields a mixing for  $\{\sigma_s, \sigma, \pi^*\}$  and  $\{\sigma_s^*, \sigma^*, \pi\}$ . We denote their respective energy eigenstates as  $\xi_{1,2,3}$  and  $\xi_{1,2,3}^*$ .

The Hamiltonian matrix for the BH-PSR molecule is block-diagonal in the hybrid basis, given by  $(H_\phi)_{\text{diag}} = \alpha^2 m_\phi \times \{A_\phi, B_\phi\} + m_\phi \times I$ . Here

$$\begin{aligned} \left. \begin{array}{l} A_\phi \\ B_\phi \end{array} \right\} &= \begin{pmatrix} -\frac{1}{8} - \epsilon & 3\epsilon^2 & 0 \\ 3\epsilon^2 & -\frac{1}{8} - \epsilon - 12\epsilon^3 & i\sqrt{2}\epsilon^{3/2} \\ 0 & -i\sqrt{2}\epsilon^{3/2} & -\frac{1}{8} - \epsilon + 6\epsilon^3 \end{pmatrix} \\ &+ \mathcal{O}(\epsilon^{-3} \exp(-1/2\epsilon)) \end{aligned} \quad (9)$$

are identical up to an exponentially-suppressed factor.  $\epsilon = \frac{r_c}{R}$  is a perturbation measure for the matrix entries. The eigenvalues are then solved to be

$$\frac{E_\xi - m_\phi}{\alpha^2 m_\phi} = A(1, 1, 1) + \left( -\sqrt{2}\epsilon^{\frac{3}{2}}, 0, \sqrt{2}\epsilon^{\frac{3}{2}} \right) + o(\epsilon^{\frac{5}{2}}) \quad (10)$$

with  $A = -\frac{1}{8} - \epsilon$ . The  $\xi_a$  and  $\xi_a^*$  profiles and their energy eigenvalues are both dependent on the BH-PSR separation. In the limit of  $R \gg r_c$  or equivalently  $\epsilon \ll 1$ , the splitting between  $E_{\xi_i^{(*)}}$  and  $E_{\xi_j^{(*)}}$  ( $i \neq j$ ) is determined by  $\sim \sqrt{2}\epsilon^{3/2}$ , while the splitting between  $E_{\xi_i}$  and  $E_{\xi_i^{(*)}}$  is exponentially suppressed. These features are demonstrated in Fig. 2. This energy-level pattern defines three characteristic time scales for this system, namely

$$T_i^+ = \frac{4\pi}{E_{\xi_i} + E_{\xi_i^*}} \sim \frac{2\pi}{m_\phi}, \quad T_{ij}^{(*)-} = \frac{4\pi}{E_{\xi_i^{(*)}} - E_{\xi_j^{(*)}}} \sim 2T_b, \quad (11)$$

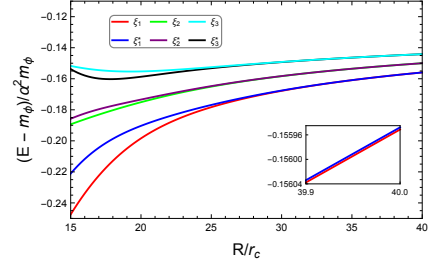


FIG. 2: Energy eigenvalues of the  $n = 2$  BH-PSR hybrid states versus the BH-PSR separation.

and exponentially-lengthened  $T_i^- = \frac{4\pi}{E_{\xi_i} - E_{\xi_i^*}}$ .

In a benchmark scenario defined by Tab. I, we find (see App. A for the details on its derivation).

$$\begin{aligned} \phi(t, \mathbf{r}) &= \frac{\sqrt{\epsilon M}}{m_\phi} \times \\ &[(-0.110C_1^+ C_1^- - 0.108C_2^+ C_2^- + 0.002C_3^+ C_3^-)s_1 + \\ &(0.110S_1^+ S_1^- - 0.108S_2^+ S_2^- + 0.002S_3^+ S_3^-)s_2 + \\ &(0.985C_1^+ C_1^- - 0.002C_2^+ C_2^- + 0.014C_3^+ C_3^-)p_{x,1} + \\ &(-0.985S_1^+ S_1^- - 0.002S_2^+ S_2^- + 0.014S_3^+ S_3^-)p_{x,2} + \\ &(0.911S_1^+ C_1^- + 0.103S_2^+ C_2^- - 0.013S_3^+ C_3^-)p_{y,1} + \\ &(-0.911C_1^+ S_1^- - 0.103C_2^+ S_2^- - 0.013C_3^+ S_3^-)p_{y,2}], \end{aligned} \quad (12)$$

where  $S_i^\pm = \sin\left(\frac{2\pi t}{T_i^\pm}\right)$  and  $C_i^\pm = \cos\left(\frac{2\pi t}{T_i^\pm}\right)$ . At  $t = 0_+$ ,  $\phi(t, \mathbf{r})$  is reduced to  $p_{x,1}$  up to a constant factor. It implies that the axion cloud is distributed near the BH initially. As time passes, the axion cloud will diffuse in the space. The PSR gets surrounded by the axion cloud massively after an evolution of  $T_3^-/4$ . As shown in Fig. 3, the axion cloud oscillates between the BH and the PSR with an approximate period of  $T_3^-$ .

$M(M_\odot)$	$\alpha$	$m_\phi(\text{eV})$	$f_\phi(\text{GeV})$	$r_c(\text{km})$	$R_0(r_c)$
2	0.015	$2 \times 10^{-12}$	$5 \times 10^{12}$	$1.3 \times 10^4$	40
$T_{b,i}(\text{s})$	$T_1^-(\text{s})$	$T_2^-(\text{s})$	$T_3^-(\text{s})$	$T_A^+(\text{s})$	$T_A^-(\text{s})$
$3.3 \times 10^3$	$1.1 \times 10^7$	$3.4 \times 10^7$	$2.1 \times 10^7$	$6.2 \times 10^3$	$3.0 \times 10^7$

TABLE I: A benchmark scenario of the BH-PSR molecule.

With the message on the axion-cloud evolution, now we are able to analyze its perturbation to the BH-PSR orbital rotation, by imposing the conditions of angular-momentum and energy conservation. For this purpose, let us define  $\beta = (R - R_0)/R_0$  and  $\gamma = (\omega - \omega_i)/\omega_i$  to characterize the perturbation. One important input is

$$[\hat{L}_{\text{AC}}, H_\phi] = \frac{-i\alpha R}{2} \left( \frac{y}{r_1^3} - \frac{y}{r_2^3} \right) \equiv T_G \neq 0. \quad (13)$$

Here  $\hat{L}_{\text{AC}} = (x\hat{p}_y - y\hat{p}_x)$  is the operator of the axion-cloud angular momentum along  $z$ -axis in the rotating reference

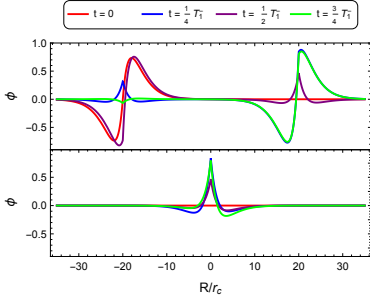


FIG. 3: Axion-cloud oscillation for a BH-PSR molecule, along  $x$ -axis (upper;  $y = z = 0$ ) and  $y$ -axis (bottom;  $x = 20r_c$ ,  $z = 0$ ).

frame, and  $T_G$  is gravitational torque. This implies that the axion cloud can interchange its angular momentum with the binary. Applying this operator to the axion field and taking an integral over the space, we find

$$L_{AC} \approx \frac{\varepsilon M}{m_\phi} \left[ 0.897 + 0.103 \cos\left(\frac{4\pi t}{T_A^+}\right) \cos\left(\frac{4\pi t}{T_A^-}\right) \right] \quad (14)$$

where  $T_A^\pm = 8\pi/[(E_{\xi_1} - E_{\xi_2}) \pm (E_{\xi_1^*} - E_{\xi_2^*})]$ . So  $L_{AC}$  is periodically reduced. Because of the conservation of angular momentum, this effect tends to decrease the binary angular velocity  $\omega$  and hence its rotational energy ( $\sim \frac{1}{4}MR^2\omega^2$ ), which in turn provides energy to induce a binary vibration, *i.e.*,  $\dot{\beta}(t) \neq 0$ . Moreover, the axion-cloud oscillation between the BH and the PSR yields a modulation to its inertia moment, which is converted to a periodic offset of rotational angular velocity between the axion cloud and the binary by Coriolis force. This effect is resolved by a variation of  $\omega$  here. In the limit of  $t \ll T_A^-$  (note  $T_A^+ \ll T_A^-$ ), eventually we find

$$\gamma(t) = -2\beta(t) = \mp 0.0026 \left(\frac{\varepsilon}{0.001}\right)^{1/2} \sin\left(\frac{2\pi t}{T_A^+}\right) + \mathcal{O}(\varepsilon), \quad (15)$$

with  $T_A^+ \sim 2T_b$  (see App. B for the details on their derivation). Notably, the magnitudes of  $\beta$  and  $\gamma$  are both  $\propto \varepsilon^{1/2}$  at the leading order, which well-justifies the adiabatic approximation taken in this study.

**Astronomical Detection** — The axion-cloud oscillation and its perturbation to the binary rotation yield unique and novel signals for detecting the BH-PSR molecules. Let us consider two PSR observables here, *i.e.*, periastron time shift and birefringence, which represent its timing and polarization observations respectively, and postpone the discussions on the GW probe to later.

The periastron time shift is a measure of the time dependence of the PSR orbital period, given by [43, 69]

$$\Delta t_P(t) = t - T_b(0) \int_0^t \frac{1}{T_b(t')} dt'. \quad (16)$$

It is modulated by the perturbation to the binary rotation, through the  $\gamma(t)$  factor in  $T_b = T_{b,i}/(1 + \gamma)$ .

Separately, the axion interaction with photons, namely  $\mathcal{L} \sim -\frac{1}{2}g_{\phi\gamma}\phi F_{\mu\nu}\tilde{F}^{\mu\nu}$ , violates parity. It thus yields a birefringence when linearly polarized light travels across an axion field [70]. Here  $F_{\mu\nu}$  is electromagnetic field strength and  $\tilde{F}_{\mu\nu}$  is its dual;  $g_{\phi\gamma} = c_\gamma\alpha_{em}/(4\pi f_a)$  is the Chern-Simon coupling, currently limited to  $< (2 \times 10^{12}\text{GeV})^{-1}$  for  $m_\phi \sim 10^{-12}\text{eV}$  [71];  $c_\gamma$  is model-dependent and can vary from one to orders higher [72–75]. The rotation of the PSR-light polarization plane is then determined by the axion profiles at the light emission (PSR) and observation (Earth) points [22, 70, 76]:

$$\Delta\Theta = g_{a\gamma} [\phi(t_{\text{ob}}, \mathbf{r}_{\text{ob}}) - \phi(t_{\text{em}}, \mathbf{r}_{\text{em}})] \approx -g_{a\gamma}\phi(t_{\text{em}}, \mathbf{r}_{\text{em}}). \quad (17)$$

We assume the Earth to be located in the  $x$ - $y$  plane for simplicity. Moreover, for  $R \gg r_c$ , the contributions of the  $s_1$ ,  $p_{x,1}$  and  $p_{y,1}$  terms in Eq. (12) are exponentially suppressed. So we have (as a reference, the current/expected precision of measuring the PSR polarization angle varies between  $\mathcal{O}(0.1^\circ - 1.0^\circ)$  [77–79])

$$\begin{aligned} \Delta\Theta \approx & \left(\frac{c_\gamma}{3 \times 10^3}\right) \left(\frac{M}{2M_\odot}\right) \left(\frac{m_\phi}{10^{-12}\text{eV}}\right)^2 \left(\frac{h_e}{500\text{km}}\right) \\ & \times [57.3^\circ S_1^+ S_1^- - 56.5^\circ S_2^+ S_2^- + 0.8^\circ S_3^+ S_3^- \\ & - 3.5^\circ S_1^+ S_1^- \cos\eta + (3.3^\circ C_1^+ S_1^- + 0.4^\circ C_2^+ S_2^-) \sin\eta], \end{aligned} \quad (18)$$

with  $\eta = \omega_i(t - \Delta t_P) \sim \frac{2\pi t}{T_b}$ . Here  $h_e$  is the emission height of the PSR light, which is usually thought to be several hundred kilometers (for a review, see [80]). This signal is then multiply modulated by the axion-cloud oscillation and the perturbed binary rotation together.

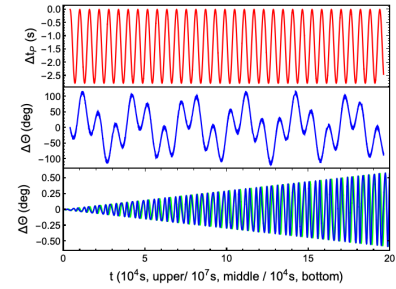


FIG. 4: Signal patterns of periastron time shift (upper) and birefringence (middle, bottom) for a BH-PSR molecule. The bottom panel is a zoom-in of the middle one at  $0_+ \leq t \ll T_A^-$ , where the  $s_2$  contributions are dropped and  $\Delta t_P$  is amplified by 300 times, for a more visual demonstration, and the reference curve (green) is drawn with  $\Delta t_P \equiv 0$  (*i.e.*,  $\eta = \omega_i t$ ).

We demonstrate the signal patterns of periastron time shift and birefringence in Fig. 4.  $\Delta t_P(t)$  oscillates with a period  $\sim T_A^+ \sim 2T_b$  and an amplitude about several seconds. Given the high precision of the relevant PSR-timing measurements [53], this signal is very promising. The signal spectrum of  $\Delta\Theta$  is shown with  $c_\gamma = 3 \times 10^3$ . Because of the dominance of the  $s_2$  contributions, this spectrum is mainly modulated by  $T_1^-$  and  $T_2^-$  through

the first two terms in Eq. (18). Moreover, a “hidden” modulation exists on top of this spectrum, due to the  $\gamma(t)$  dependence of the  $\eta$  (or  $T_b$ ) parameter. This modulation is manifested as an offset between the blue and green curves in the bottom panel, with a period  $\sim T_A^+$  and an amplitude  $\sim |\Delta t_P|$ . It is exactly the effect measured by the periastron time shift. These two observables thus can be correlated to strengthen the detection!

**Conclusion and Outlook** — In this letter, we develop a semi-analytical formalism to analyze the orbital hybridization of a BH-PSR gravitational molecule and its state evolution, using the LCAO method with a Born-Oppenheimer approximation. An oscillating axion-cloud profile and a perturbed binary rotation are then predicted for this molecule, together with unique and novel detection signals. Following this work, we can see several important directions to explore.

First, draw a full picture on gravitational molecules, with refined methods. Despite their rich physics, we consider mainly a BH-PSR molecule with  $M_{\text{BH}} = M_{\text{PSR}}$  so far. Generalizing this study to other possibilities, such as a variance of the analyzed one in terms of BH mass ( $M_{\text{BH}} \neq M_{\text{PSR}}$ ),  $\alpha$  value, spin orientation, initial state, orbit eccentricity, saturation condition, Bosenova constraint, etc., is naturally expected. If the BH and its companion have a different mass, *e.g.*, the orbital hybridization may get weakened (if no energy-level degeneracy occurs near the initial state). To compensate for this effect, relatively small  $R_0$  values might be needed. Separately, turning off the Bosenova constraint may increase the amount of the bosonic matter transferred between the BH and its companion, and hence enhance the strength of the relevant signals. One can also extend this study to more complex systems such as three-body molecules. To broaden the exploration scope and improve the analysis precision, notably, it will be important to combine this analysis formalism with a refined numerical method.

Second, explore the multi-messenger signals of gravitational molecules. Novel physics often yields unique detection signals. Here we propose two PSR observables, representing its timing and polarization measurements respectively, for detecting the BH-PSR molecules. Complementarily, the GW probe can play a role. Distinguishable signals may arise from, *e.g.*, resonant energy-level transitions and late-time inspiral evolution (especially for large  $\alpha$ ), with an imprint left by the molecule evolution. A natural question is then whether a correlation in pattern or some other formats exists for the GW and electromagnetic signals, as it does for the PSR timing and polarization observables. At last, we should be aware that gravitational molecules can be a laboratory for studying ultralight bosons other than axions, such as dark photons and massive gravitons. Physics relying on the nature of these particles has been noticed in the studies on gravitational atoms [38, 81–84]. We leave the exploration of these interesting topics to a future work.

## ACKNOWLEDGEMENT

We would thank Ding Pan for useful discussions on the first-principle calculations, Xuhui Huang, Fu Kit Sheong and Jingxuan Zhang on the electronic structure of the  $H_2^+$  ion (used for our method testing), and Ding Pan, Xi Tong and Yi Wang for valuable comments on this manuscript. This work is supported by the Collaborative Research Fund under Grant No. C6017-20G which is issued by the Research Grants Council of Hong Kong S.A.R.

## APPENDIX A. ORBITAL HYBRIDIZATION OF THE BH-PSR MOLECULE

In the hybrid basis, namely  $(\sigma_s, \sigma, \pi^*, \sigma_s^*, \sigma^*, \pi)^T$ , the Hamiltonian matrix of the considered BH-PSR molecule is block-diagonal:

$$\frac{H_\phi - m_\phi \times I}{\alpha^2 m_\phi} = \begin{pmatrix} A_\phi & \\ & B_\phi \end{pmatrix}, \quad (19)$$

where

$$A_\phi = \begin{pmatrix} -0.150001 & 0.001879 & 0 \\ 0.001879 & -0.150188 & -0.005590i \\ 0 & 0.005590i & -0.149906 \end{pmatrix} \quad (20)$$

and

$$B_\phi = \begin{pmatrix} -0.149999 & 0.001871 & 0 \\ 0.001871 & -0.150187 & -0.005590i \\ 0 & 0.005590i & -0.149906 \end{pmatrix}. \quad (21)$$

Their respective eigenvalues and eigenstates are then solved to be

$$\begin{aligned} \frac{E_\xi - m_\phi}{\alpha^2 m_\phi} &= (-0.155951, -0.149990, -0.144153) \\ \frac{E_{\xi^*} - m_\phi}{\alpha^2 m_\phi} &= (-0.155948, -0.149991, -0.144155), \end{aligned} \quad (22)$$

and

$$V_\xi = \begin{pmatrix} \xi_1 \\ \xi_2 \\ \xi_3 \end{pmatrix} = \underbrace{\begin{pmatrix} -0.22587 & 0.71522 & 0.66140i \\ -0.947919 & -0.00485 & -0.31847i \\ 0.22457 & 0.69889 & -0.67906i \end{pmatrix}}_{U_A} \begin{pmatrix} \sigma_s \\ \sigma \\ \pi^* \end{pmatrix} \quad (23)$$

$$V_{\xi^*} = \begin{pmatrix} \xi_1^* \\ \xi_2^* \\ \xi_3^* \end{pmatrix} = \underbrace{\begin{pmatrix} -0.22493 & 0.71518 & 0.66176i \\ -0.94834 & -0.00474 & -0.31721i \\ 0.22373 & 0.69892 & -0.67930i \end{pmatrix}}_{U_B} \begin{pmatrix} \sigma_s^* \\ \sigma^* \\ \pi \end{pmatrix}. \quad (24)$$

Denoting

$$V_h = \begin{pmatrix} \sigma_s \\ \sigma \\ \pi^* \end{pmatrix}, \quad V_{h^*} = \begin{pmatrix} \sigma_s^* \\ \sigma^* \\ \pi \end{pmatrix}, \quad (25)$$

we can decompose the axion initial state as

$$\begin{aligned} |211, 1\rangle &= C^T V_h + C^{*T} V_{h^*} \\ &= C^T U_A^{-1} V_\xi + C^{*T} U_B^{-1} V_{\xi^*}, \end{aligned} \quad (26)$$

where

$$\begin{aligned} C_A^T &= \frac{1}{2\sqrt{2}} \begin{pmatrix} 0 & 1 & i \\ A_\sigma & A_{\pi^*} & \end{pmatrix}, \\ C_{A^*}^T &= \frac{1}{2\sqrt{2}} \begin{pmatrix} 0 & 1 & i \\ A_{\sigma^*} & A_\pi & \end{pmatrix}. \end{aligned} \quad (27)$$

Then the complex axion field evolves as

$$\begin{aligned} \psi(t, \mathbf{r}) &= \sum_{i=1}^3 (C^T U_A^{-1})_i (V_\xi)_i \exp[-iE_{\xi_i} t] \\ &+ \sum_{i=1}^3 (C^{*T} U_B^{-1})_i (V_{\xi^*})_i \exp[-iE_{\xi_i^*} t]. \end{aligned} \quad (28)$$

Then replacing  $V_\xi$  and  $V_{\xi^*}$  with Eq. (23-24) and Eq. (6) in sequence, we find

$$\begin{aligned} \phi(t, \mathbf{r}) &= \frac{1}{\sqrt{2m_\phi}} [\psi(t, \mathbf{r}) + \psi^*(t, \mathbf{r})] = \frac{\sqrt{\varepsilon M}}{m_\phi} \times \\ &[(-0.110C_1^+ C_1^- - 0.108C_2^+ C_2^- + 0.002C_3^+ C_3^-)s_1 + \\ &(0.110S_1^+ S_1^- - 0.108S_2^+ S_2^- + 0.002S_3^+ S_3^-)s_2 + \\ &(0.985C_1^+ C_1^- - 0.002C_2^+ C_2^- + 0.014C_3^+ C_3^-)p_{x,1} + \\ &(-0.985S_1^+ S_1^- - 0.002S_2^+ S_2^- + 0.014S_3^+ S_3^-)p_{x,2} + \\ &(0.911S_1^+ C_1^- + 0.103S_2^+ C_2^- - 0.013S_3^+ C_3^-)p_{y,1} + \\ &(-0.911C_1^+ S_1^- - 0.103C_2^+ S_2^- - 0.013C_3^+ S_3^-)p_{y,2}], \end{aligned} \quad (29)$$

where  $S_i^\pm = \sin\left(\frac{2\pi t}{T_i^\pm}\right)$  and  $C_i^\pm = \cos\left(\frac{2\pi t}{T_i^\pm}\right)$ , with  $T_i^\pm = 4\pi/|E_{\xi_i} \pm E_{\xi_i^*}|$ . Please note that the eigenvalues and eigenstates of  $\hat{H}_\phi$  and hence  $\phi(t, \mathbf{r})$  can be directly solved in the atomic basis of this molecule. Here we work in the hybrid basis first and then convert the solutions to the ones in the atomic basis simply for the convenience of discussions.

## APPENDIX B. PERTURBATION TO THE BH-PSR ROTATION

Below we will analyze the perturbation of the axion-cloud evolution to the BH-PSR rotation, by imposing the conditions of angular-momentum and energy conservation. We will use the adiabatic measure, namely

$\varepsilon = M_{AC}/M$ , as the perturbation parameter, and work in the laboratory reference frame.

At  $t = 0_+$ , the PSR and the BH are located at  $\{x = \pm \frac{R_0}{2}(1 \pm \frac{\varepsilon}{2}), y = z = 0\}$ , with an angular velocity

$$\omega_i = \omega(t = 0_+) = \frac{1}{R_0} \left(\frac{2GM}{R_0}\right)^{1/2} \left(1 + \frac{\varepsilon}{4}\right). \quad (30)$$

The BH-PSR binary thus has an initial orbital angular momentum

$$\begin{aligned} L_{b,i} &= M \left\{ \left[\frac{R_0}{2} \left(1 + \frac{\varepsilon}{2}\right)\right]^2 + \left[\frac{R_0}{2} \left(1 - \frac{\varepsilon}{2}\right)\right]^2 \right\} \omega_i \\ &= M \left(\frac{GM R_0}{2}\right)^{1/2} \left(1 + \frac{\varepsilon}{4}\right) \\ &\propto \frac{M}{m_\phi} \left(1 + \frac{\varepsilon}{4}\right). \end{aligned} \quad (31)$$

It represents a leading-order contribution to the total angular momentum.

The axion cloud has two contributions to the total angular momentum. Both of them arise from the order of  $\mathcal{O}(\varepsilon)$ . The first one is from the axion-cloud rotation around the binary mass center (in the rotating reference frame). It is given by

$$L_{AC} = - \int d^3\vec{x} \frac{d\phi}{dt} \left( x \frac{\partial}{\partial y} - y \frac{\partial}{\partial x} \right) \phi = \frac{\varepsilon M}{m_\phi} X_{AC}(t), \quad (32)$$

where

$$\begin{aligned} X_{AC} &\approx \frac{1}{m_\phi} \left[ 0.448 (E_{\xi_3} + E_{\xi_3^*}) + 0.026 (E_{\xi_1} + E_{\xi_2}) \right. \\ &\quad \left. \times \cos\left(\frac{4\pi t}{T_{12}^-}\right) + 0.024 (E_{\xi_1^*} + E_{\xi_2^*}) \cos\left(\frac{4\pi t}{T_{12^*}^-}\right) \right] \\ &= 0.897 + 0.051 \cos\left(\frac{4\pi t}{T_{12}^-}\right) + 0.051 \cos\left(\frac{4\pi t}{T_{12^*}^-}\right) \\ &= 0.897 + 0.103 \cos\left(\frac{4\pi t}{T_A^+}\right) \cos\left(\frac{4\pi t}{T_A^-}\right), \end{aligned} \quad (33)$$

with  $T_{ij}^\pm = 4\pi/(E_{\xi_i} \pm E_{\xi_j})$ ,  $T_{ij^*}^\pm = 4\pi/(E_{\xi_i^*} \pm E_{\xi_j^*})$  and  $T_A^\pm = 8\pi/[(E_{\xi_1} - E_{\xi_2}) \pm (E_{\xi_1^*} - E_{\xi_2^*})]$ . In deriving Eq. (33) we leave out the terms which are either suppressed by the coefficients of the  $T_1^\pm$ -related terms in Eq. (12) or are proportional to the energy gap  $E_{\xi_i^{(*)}} - E_{\xi_j^{(*)}}$ . We also apply  $E_{\xi_i^{(*)}} \approx m_\phi$  to obtain the result in the last line.

The second contribution of the axion cloud is induced by the binary rotation. It is a product of the binary angular velocity  $\omega$  and the axion-cloud inertia moment  $I(t)$  w.r.t. the  $z$ -axis. Here  $I(t)$  is given by

$$\begin{aligned} I(t) &= \int d^3\vec{x} m_\phi^2 \phi^2 (r \sin\theta)^2 \\ &\approx I_i \left[ 0.915 + 0.084 \cos\left(\frac{4\pi t}{T_A^+}\right) \cos\left(\frac{4\pi t}{T_A^-}\right) \right], \end{aligned} \quad (34)$$

with

$$I_i = \frac{\varepsilon M}{\alpha^2 m_\phi^2} \left[ 24 + \frac{1}{4} \left( \frac{R_0}{r_c} \right)^2 \right] \quad (35)$$

being the rotational inertia at  $t = 0_+$ . The contributions from the  $V_i$  and  $V_c$  terms have been neglected, due to a suppression of  $\alpha^2$ . We thus have the orbital angular momentum at the order of  $\sim \mathcal{O}(\varepsilon)$

$$L_{\text{AO}} = I\omega = I\omega_i = \sqrt{2}m_\phi \frac{\alpha^2 I}{(R/r_c)^{3/2}} = \frac{\varepsilon M}{m_\phi} X_{\text{AO}}, \quad (36)$$

with

$$X_{\text{AO}} = 2.17 + 0.20 \cos\left(\frac{4\pi t}{T_A^+}\right) \cos\left(\frac{4\pi t}{T_A^-}\right). \quad (37)$$

With these inputs, we are able to write down the condition of angular-momentum conservation

$$\begin{aligned} L_{b,i} + \frac{\varepsilon M}{m_\phi} (X_{\text{AO},i} - X_{\text{AC},i}) \\ = \frac{1}{2} MR^2 \omega + \frac{\varepsilon M}{m_\phi} (X_{\text{AO}} - X_{\text{AC}}), \end{aligned} \quad (38)$$

and the condition of energy conservation

$$\begin{aligned} \frac{1}{4} MR_0^2 \omega_i^2 - \frac{GM^2}{R_0} + \varepsilon \frac{M}{m_\phi} \langle E_\phi \rangle_i + \frac{1}{2} I_i \omega_i^2 \\ = \frac{1}{4} M (\dot{R}^2 + R^2 \omega^2) - \frac{GM^2}{R} + \varepsilon \frac{M}{m_\phi} \langle E_\phi \rangle(t) \\ + \frac{1}{2} I(t) \left( \omega^2 + \frac{\dot{R}^2}{R^2} \right), \end{aligned} \quad (39)$$

at the order of  $\mathcal{O}(\varepsilon)$ , for the molecule evolution, where  $\langle E_\phi \rangle$  is the mean of the axion energy. The BH spin couples to these two equations at a high order of  $\alpha$  only and hence has been neglected here. A dimensional analysis indicates that all terms are  $\propto \frac{M}{m_\phi}$  in Eq. (38), and  $\propto G^2 M^3 m_\phi^2$  in Eq. (39). Notably, the modulation of  $I(t)$  in Eq. (35) is expected to be converted to a periodic offset of rotational angular velocity between the axion cloud and the binary by Coriolis force. Here we have implicitly assumed that in the adiabatic limit this offset will be quickly resolved by a variance of  $\omega$  such that the binary and the axion-cloud orbital rotations are always aligned.

These two equations can be rewritten as

$$\omega = \left( \frac{MR^2}{2} \right)^{-1} \left[ \frac{MR_0^2}{2} \omega_i - \frac{\varepsilon M}{m_\phi} (\Delta X_{\text{AO}} - \Delta X_{\text{AC}}) \right] \quad (40)$$

and

$$\dot{\beta}^2 + \frac{2GM}{R_0^3} \beta^2 = \frac{2^{5/2} \varepsilon}{m_\phi R_0^3} \left( \frac{GM}{R_0} \right)^{1/2} \left( \frac{\Delta X_{\text{AO}}}{2} - \Delta X_{\text{AC}} \right), \quad (41)$$

with  $\Delta X = X(t) - X_i$  and  $\beta(t) = \frac{R}{R_0} - 1$ . Eventually in the limit of  $t \ll T_A^-$  (note  $T_A^+ \ll T_A^-$ ) we find

$$\begin{aligned} \beta(t) &= \pm \left[ \frac{0.005 \times 2^{3/2} \varepsilon \sqrt{GM}}{m_\phi R_0^{7/2} \left( \frac{2GM}{R_0^3} - \left( \frac{2\pi}{T_A^+} \right)^2 \right)} \right]^{1/2} \sin\left(\frac{2\pi t}{T_A^+}\right) \\ &\quad + \mathcal{O}(\varepsilon) \\ &= \pm \left[ \frac{0.010 \varepsilon}{(R_0/r_c)^{1/2}} \right]^{1/2} \sin\left(\frac{2\pi t}{T_A^+}\right) + \mathcal{O}(\varepsilon) \\ &= \pm 0.0013 \left( \frac{\varepsilon}{0.001} \right)^{1/2} \sin\left(\frac{2\pi t}{T_A^+}\right) + \mathcal{O}(\varepsilon), \end{aligned} \quad (42)$$

and

$$\gamma(t) = \frac{\omega(t)}{\omega_i} - 1 = -2\beta(t) + \mathcal{O}(\varepsilon). \quad (43)$$

In the second line of Eq. (42), the relation

$$T_A^+ = 2\pi \left( \frac{2m_\phi R_0^3}{\alpha} \right)^{1/2} \quad (44)$$

has been applied.

---

\* Electronic address: taoliu@ust.hk

† Electronic address: klyuaa@connect.ust.hk

- [1] T. Damour, N. Deruelle, and R. Ruffini, *Lett. Nuovo Cim.* **15**, 257 (1976).
- [2] J. D. Bekenstein, *Phys. Rev. D* **7**, 949 (1973).
- [3] J. D. Bekenstein and M. Schiffer, *Phys. Rev. D* **58**, 064014 (1998), gr-qc/9803033.
- [4] R. Brito, V. Cardoso, and P. Pani, *Lect. Notes Phys.* **906**, pp.1 (2015), 1501.06570.
- [5] D. R. Brill, P. L. Chrzanowski, C. Martin Pereira, E. D. Fackerell, and J. R. Ipser, *Phys. Rev. D* **5**, 1913 (1972).
- [6] J. G. Rosa, *JHEP* **06**, 015 (2010), 0912.1780.
- [7] S. L. Detweiler, *Phys. Rev. D* **22**, 2323 (1980).
- [8] S. R. Dolan, *Phys. Rev. D* **76**, 084001 (2007), 0705.2880.
- [9] S. Endlich and R. Penco, *JHEP* **05**, 052 (2017), 1609.06723.
- [10] H. Yoshino and H. Kodama, *PTEP* **2014**, 043E02 (2014), 1312.2326.
- [11] A. Arvanitaki and S. Dubovsky, *Phys. Rev. D* **83**, 044026 (2011), 1004.3558.
- [12] R. Peccei and H. R. Quinn, *Phys. Rev. Lett.* **38**, 1440 (1977).
- [13] R. Peccei and H. R. Quinn, *Phys. Rev. D* **16**, 1791 (1977).
- [14] S. Weinberg, *Phys. Rev. Lett.* **40**, 223 (1978).
- [15] F. Wilczek, *Phys. Rev. Lett.* **40**, 279 (1978).
- [16] M. Dine and W. Fischler, *Phys. Lett. B* **120**, 137 (1983).
- [17] J. Preskill, M. B. Wise, and F. Wilczek, *Phys. Lett. B* **120**, 127 (1983).
- [18] L. F. Abbott and P. Sikivie, *Phys. Lett. B* **120**, 133 (1983).
- [19] A. Arvanitaki, S. Dimopoulos, S. Dubovsky, N. Kaloper, and J. March-Russell, *Phys. Rev. D* **81**, 123530 (2010), 0905.4720.

- [20] P. Svrcek and E. Witten, *JHEP* **06**, 051 (2006), hep-th/0605206.
- [21] M. Cicoli, M. Goodsell, and A. Ringwald, *JHEP* **10**, 146 (2012), 1206.0819.
- [22] D. J. E. Marsh, *Phys. Rept.* **643**, 1 (2016), 1510.07633.
- [23] I. G. Irastorza and J. Redondo, *Prog. Part. Nucl. Phys.* **102**, 89 (2018), 1801.08127.
- [24] R. Brito, S. Ghosh, E. Barausse, E. Berti, V. Cardoso, I. Dvorkin, A. Klein, and P. Pani, *Phys. Rev. Lett.* **119**, 131101 (2017), 1706.05097.
- [25] Y. Chen, J. Shu, X. Xue, Q. Yuan, and Y. Zhao, *Phys. Rev. Lett.* **124**, 061102 (2020), 1905.02213.
- [26] H. Davoudiasl and P. B. Denton, *Phys. Rev. Lett.* **123**, 021102 (2019), 1904.09242.
- [27] A. D. Plascencia and A. Urbano, *JCAP* **04**, 059 (2018), 1711.08298.
- [28] M. Isi, L. Sun, R. Brito, and A. Melatos, *Phys. Rev. D* **99**, 084042 (2019), [Erratum: *Phys.Rev.D* 102, 049901 (2020)], 1810.03812.
- [29] W. E. East, *Phys. Rev. Lett.* **121**, 131104 (2018), 1807.00043.
- [30] D. J. E. Marsh and S. Hoof (2021), 2106.08797.
- [31] C. Yuan, R. Brito, and V. Cardoso (2021), 2106.00021.
- [32] M. Baryakhtar, M. Galanis, R. Lasenby, and O. Simon, *Phys. Rev. D* **103**, 095019 (2021), 2011.11646.
- [33] K. K. Y. Ng, S. Vitale, O. A. Hannuksela, and T. G. F. Li, *Phys. Rev. Lett.* **126**, 151102 (2021), 2011.06010.
- [34] K. K. Y. Ng, M. Isi, C.-J. Haster, and S. Vitale, *Phys. Rev. D* **102**, 083020 (2020), 2007.12793.
- [35] M. Kavic, S. L. Liebling, M. Lippert, and J. H. Simonetti, *JCAP* **08**, 005 (2020), 1910.06977.
- [36] S. Wen, P. G. Jonker, N. C. Stone, and A. I. Zabludoff (2021), 2104.01498.
- [37] H. S. Chia, Ph.D. thesis, Amsterdam U. (2020), 2012.09167.
- [38] N. Siemonsen and W. E. East, *Phys. Rev. D* **101**, 024019 (2020), 1910.09476.
- [39] S. Ghosh, E. Berti, R. Brito, and M. Richartz, *Phys. Rev. D* **99**, 104030 (2019), 1812.01620.
- [40] J. Zhang and H. Yang, *Phys. Rev. D* **101**, 043020 (2020), 1907.13582.
- [41] N. Fernandez, A. Ghalsasi, and S. Profumo (2019), 1911.07862.
- [42] D. Baumann, H. S. Chia, and R. A. Porto, *Phys. Rev. D* **99**, 044001 (2019), 1804.03208.
- [43] Q. Ding, X. Tong, and Y. Wang, *Astrophys. J.* **908**, 78 (2021), 2009.11106.
- [44] D. Baumann, H. S. Chia, J. Stout, and L. ter Haar, *JCAP* **12**, 006 (2019), 1908.10370.
- [45] D. Baumann, H. S. Chia, R. A. Porto, and J. Stout, *Phys. Rev. D* **101**, 083019 (2020), 1912.04932.
- [46] X. Tong, Y. Wang, and H.-Y. Zhu (2021), 2106.13484.
- [47] T. Ikeda, L. Bernard, V. Cardoso, and M. Zilhão, *Phys. Rev. D* **103**, 024020 (2021), 2010.00008.
- [48] D. Chattopadhyay, S. Stevenson, J. R. Hurley, M. Bailes, and F. Broekgaarden, *Mon. Not. Roy. Astron. Soc.* **504**, 3682 (2021), 2011.13503.
- [49] Y. Shao and X.-D. Li, *Mon. Not. Roy. Astron. Soc.* **477**, L128 (2018), 1804.06014.
- [50] Y. Shao and X.-D. Li (2021), 2107.03565.
- [51] J. H. Taylor and J. M. Weisberg, *Astrophys. J.* **253**, 908 (1982).
- [52] J. H. Taylor and J. M. Weisberg, *Astrophys. J.* **345**, 434 (1989).
- [53] J. M. Weisberg, D. J. Nice, and J. H. Taylor, *Astrophys. J.* **722**, 1030 (2010), 1011.0718.
- [54] *Molecular orbital theory*, <https://chem.libretexts.org/@go/page/20791>.
- [55] M. Valtonen and H. Karttunen, *The Three-Body Problem* (2006).
- [56] J. G. Hills, *Monthly Notices of the Royal Astronomical Society* **175**, 1P (1976), ISSN 0035-8711.
- [57] G. W. Clark, *apjl* **199**, L143 (1975).
- [58] T. R. Stoeckley, in *Bulletin of the American Astronomical Society* (1981), vol. 13, pp. 256–259.
- [59] D. C. Hoggie, *IAU Symp.* **208**, 81 (2003), astro-ph/0111045.
- [60] J. G. Hills and L. W. Fullerton, *Astron. J.* **85:9**, 1281 (1980).
- [61] B. M. Ziosi, M. Mapelli, M. Branchesi, and G. Tormen, *Mon. Not. Roy. Astron. Soc.* **441**, 3703 (2014), 1404.7147.
- [62] M. Celoria, R. Oliveri, A. Sesana, and M. Mapelli (2018), 1807.11489.
- [63] M. Colpi, P. Casella, V. Gorini, U. Moschella, and A. Posenti, *Physics of Relativistic Objects in Compact Binaries: From Birth to Coalescence*, vol. 359 (2009), ISBN 978-1-4020-9263-3.
- [64] H. Yoshino and H. Kodama, *Prog. Theor. Phys.* **128**, 153 (2012), 1203.5070.
- [65] A. Arvanitaki, M. Baryakhtar, and X. Huang, *Phys. Rev. D* **91**, 084011 (2015), 1411.2263.
- [66] J. Anandan and J. Suzuki (2003), quant-ph/0305081.
- [67] J. J. Sakurai, *Phys. Rev. D* **21**, 2993 (1980).
- [68] H. Johnston, *Lecture notes: Senior astrophysics*, <http://www.physics.usyd.edu.au/~helenj/SeniorAstro/lecture11.pdf> (2018).
- [69] J. H. Taylor, *Rev. Mod. Phys.* **66**, 711 (1994).
- [70] S. M. Carroll, G. B. Field, and R. Jackiw, *Phys. Rev. D* **41**, 1231 (1990).
- [71] M. Tanabashi et al. (Particle Data Group), *Phys. Rev. D* **98**, 030001 (2018).
- [72] K. Choi and S. H. Im, *JHEP* **01**, 149 (2016), 1511.00132.
- [73] D. E. Kaplan and R. Rattazzi, *Phys. Rev. D* **93**, 085007 (2016), 1511.01827.
- [74] A. J. Long, *JHEP* **07**, 066 (2018), 1803.07086.
- [75] P. Agrawal, J. Fan, M. Reece, and L.-T. Wang, *JHEP* **02**, 006 (2018), 1709.06085.
- [76] D. Harari and P. Sikivie, *Phys. Lett. B* **289**, 67 (1992).
- [77] V. Tatischeff, A. De Angelis, C. Gouiffès, L. Hanlon, P. Laurent, G. M. Madejski, M. Tavani, and A. Uliyanov (e-ASTROGAM), *J. Astron. Telesc. Instrum. Syst.* **4**, 011003 (2017), 1706.07031.
- [78] A. Slowikowska, G. Kanbach, M. Kramer, and A. Stefanescu, *Monthly Notices of the Royal Astronomical Society* **397**, 103 (2009), ISSN 0035-8711.
- [79] P. Moran, A. Shearer, R. Mignani, A. Slowikowska, A. De Luca, C. Gouiffès, and P. Laurent, *Mon. Not. Roy. Astron. Soc.* **433**, 2564 (2013), 1305.6824.
- [80] D. Mitra, *J. Astrophys. Astron.* **38**, 52 (2017), 1709.07179.
- [81] M. Baryakhtar, R. Lasenby, and M. Teo, *Phys. Rev. D* **96**, 035019 (2017), 1704.05081.
- [82] R. Brito, S. Grillo, and P. Pani, *Phys. Rev. Lett.* **124**, 211101 (2020), 2002.04055.
- [83] A. Caputo, S. J. Witte, D. Blas, and P. Pani (2021), 2102.11280.
- [84] V. Cardoso, P. Pani, and T.-T. Yu, *Phys. Rev. D* **95**, 124056 (2017), 1704.06151.